This is Chapter 1 "Introduction" from my PhD thesis

Kluckner, A. 2023. Tunnelling at greater depths: Study on the ground and system behaviour when passing a stiff rock block in a weak zone. PhD thesis. Graz University of Technology, Graz, Austria.

The full thesis can be downloaded from the TU Graz repository: LINK

If you have any questions or remarks, you can contact me on

ResearchGate: LINK

or on

LinkedIn: LINK.

Enjoy reading.

Best regards, Alexander Kluckner



Dipl.-Ing. Alexander Kluckner, BSc

Tunnelling at greater depths: Study on the ground and system behaviour when passing a stiff rock block in a weak zone

DOCTORAL THESIS

to achieve the university degree of Doktor der technischen Wissenschaften

submitted to

Graz University of Technology

Reviewers

Em.Univ.-Prof. Dipl.-Ing. Dr.mont. Wulf Schubert Faculty of Civil Engineering Sciences Graz University of Technology, Graz, Austria

Univ.-Prof. Dr. Nobuharu Isago Faculty of Urban Environmental Sciences Tokyo Metropolitan University, Tokyo, Japan

Abstract

Title: Tunnelling at greater depths: Study on the ground and system behaviour when passing a stiff rock block in a weak zone

Keywords: deep tunnelling, conventional, brittle fault zone, block-in-matrix, stiff block, shear bands

A stiff block in brittle, weak fault zones can lead to unfavourable ground behaviour when being approached by a tunnel drive. It attracts stresses and may fail when it is close to the tunnel face endangering the tunnel stability. The thesis investigates the ground behaviour with a quasi-two-dimensional parametric study. The tunnel diameter is 10 m, the block height is 2 m, 5 m, or 10 m, and the distance between the block and the tunnel is 1 m, 5 m, or 10 m. One critical case is analysed in three dimensions. Another study simulates a real tunnel drive that crosses a block with a height of over 25 m. Strain data from a lining segment measured at the construction site with a distributed fibre optic sensing system is used to set up the Burgers-Mohr model simulating the shotcrete material behaviour. All simulations consider an interface between the block and the matrix material. From the block, shear bands form towards the tunnel. In the parametric study, even if the block-matrix stiffness contrast is high or the block is close to the tunnel, differences in the tunnel displacements between cases with block and related cases without block are little. Of the cases analysed, those with a hydrostatic primary stress state are least favourable. If the primary stresses are anisotropic, the effect of the block on the ground behaviour strongly depends on the block distance. The case study suggests that the block must be not too high to be hazardous if it fails. Otherwise, stresses redistributed because of the tunnel drive cannot concentrate at the block's top and bottom. In case the stresses are high enough at the moment of block failure, large-scale shear failure of the rock mass close to the tunnel may occur. If the location of blocks is unknown, state-of-the-art approaches to evaluate tunnel displacements must be applied to increase the probability of identifying blocks in time during tunnelling. Making the system stiffer of less stiff (e.g., by adapting the moment of ring closure) may not lead to a less hazardous situation. It is advised to minimise the unreinforced rock mass volume close to the tunnel face to prevent shear bands from reaching the tunnel.

Contents

Li	st of	Figures	xxi
Li	st of	Tables	xxix
Li	st of	Acronyms, Symbols, and Notations	xxxv
1	Intr	roduction	1
	1.1	Research motivation	. 1
	1.2	Research questions	. 4
	1.3	Methodology	. 5
	1.4	Thesis structure and objectives	. 6
	1.5	Research limitations	. 7
2	Abo	out fault zones and block-in-matrix rocks	9
	2.1	Brittle fault zones	. 12
	2.2	Block-in-matrix rocks	. 14
3	Son	ne properties of rocks and rock masses	19
	3.1	Geometric properties of bimrock blocks	. 19
		3.1.1 Block shape	. 19
		3.1.2 Block location and orientation	. 21
		3.1.3 Block size	. 21
	3.2	Mechanical properties of rocks and rock masses	. 22
		3.2.1 Shear strength of the matrix material	. 22
		3.2.2 Uniaxial compressive strength of the matrix material	. 28
		3.2.3 Shear strength of the block material	. 28
		3.2.4 Uniaxial compressive strength of the block material $\ \ldots \ \ldots \ \ldots$. 28
		3.2.5 Tensile strength	. 30
		3.2.6 Dilation angle	. 32
		3.2.7 Poisson's ratio	. 33
		3.2.8 Density	. 36
		3.2.9 Young's modulus	. 36
		3.2.10 Block-matrix contacts	. 40
4	Son	ne characteristics of shotcrete	45
	4.1	Hardening of concrete	. 47
	4.2	Origin of strength and stiffness growth	. 47
	4.3	A note on the behaviour under pressure	. 48
	4.4	About strain in shotcreted tunnel linings	. 49
	15	Postroints	50

CONTENTS

	4.6	Strain	n components	51
		4.6.1	Elastic (instantaneous) strain	52
		4.6.2	Thermal elastic (instantaneous) strain	52
		4.6.3	Shrinkage (delayed) strain	54
		4.6.4	Creep (delayed) strain	57
		4.6.5	Plastic (instantaneous) strain	60
		4.6.6	Irrecoverable strain due to ageing	62
	4.7	Peak	strain	62
	4.8	Shotc	rete strength	63
	4.9	Shotc	rete deformability	66
		4.9.1	Poisson's ratio	67
		4.9.2	Empirical approximation	67
5	The	ermo-cl	nemo-mechanical shotcrete model	69
	5.1	Displa	acement and strain field	70
	5.2	Shotc	rete model	71
		5.2.1	Chemo-thermal coupling	73
		5.2.2	Thermo-mechanical coupling $\ldots \ldots \ldots \ldots \ldots \ldots$	74
		5.2.3	Chemo-mechanical coupling	74
6	Stif	f block	next to excavation (2D): Parametric study	81
	6.1	Nume	erical model setup	82
		6.1.1	Modelling of system features	82
		6.1.2	Modelling of material behaviour	84
		6.1.3	$\operatorname{Mesh} \ldots \ldots$	86
		6.1.4	$\label{eq:Model size of Model size} Model size$	87
		6.1.5	Boundary conditions and initial state	87
		6.1.6	Solve criterion and damping	87
		6.1.7	Excavation method	88
	6.2	Nume	erical input parameters	89
		6.2.1	Tunnel shape and size \hdots	90
		6.2.2	Primary stress state	90
		6.2.3	Block shape	90
		6.2.4	Block location and orientation \dots	90
		6.2.5	Distance of the block from the tunnel and block size $\ \ldots \ \ldots \ \ldots$	94
		6.2.6	Internal angle of friction of the matrix material	94
		6.2.7	Internal angle of friction of the block material	94
		6.2.8	Cohesion of the matrix material	95
		6.2.9	Uniaxial compressive strength of the matrix material	96
		6.2.10	Uniaxial compressive strength of the block material	97
		6.2.11	Cohesion of the block material	98
		6.2.12	Tensile strength	98
		6.2.13	Dilation angle	100
		6.2.14	Poisson's ratio	100
		6.2.15	Density	100
		6.2.16	Young's modulus	100
		6 2 17	Interface properties	101

CONTENTS xv

	6.3	Evalu	ation approach	103
		6.3.1	Angular deviation of in-plane tunnel displacement vectors	105
		6.3.2	Total in-plane tunnel displacements	107
		6.3.3	Shear strain increment along tunnel periphery	108
		6.3.4	Maximum in-plane block-matrix interface slip, and other interface related	
			variables	109
		6.3.5	Block bending	109
		6.3.6	Horizontal evaluation plane	
		6.3.7	Path of highest secondary in-plane major principal stresses	
		6.3.8	Parameter development with ongoing relaxation	
		6.3.9	Zone-by-zone comparison of different cases	
			Orientation of stresses along block periphery	
			Spalling limit and damage threshold	
			Work	
	6.4		ts: Summary	
	0.1	6.4.1	In-plane block-matrix interface slip	
		6.4.2	Shear strain increment	
		6.4.3	Block deformation	
		6.4.4	Block displacement	
		6.4.5	Path of the highest secondary in-plane major principal stresses	
		6.4.6	Shear strain increment along tunnel periphery	
		6.4.7	Displacement of the tunnel periphery	
		6.4.8	Yielded zones	
		6.4.9	Block failure	
			In-plane stresses	
			Orientation of in-plane stresses	
			Elastic work	
	6.5		pretation and discussion	
	0.0	6.5.1	The block-matrix interface rules	
		0.0.1		
		6.5.2	•	
		6.5.3	Small block distance: hazardous	
		6.5.4	Identification on site? It depends	
		6.5.5	Underestimation of the situation	
		6.5.6	About installing support	157
		6.5.7	On dynamic effects	
		6.5.8	Most probable scenario	158
7	Stiff	f block	next to excavation (3D): Supplementary study	159
	7.1		erical model setup	159
		7.1.1	Modelling of system features	159
		7.1.2	Mesh	160
		7.1.3	Model size	160
		7.1.4	Boundary conditions and initial state	
		7.1.5	Construction sequence and excavation method	
	7.2		erical input parameters	161
		7.2.1	Block shape	161
		7.2.2	Block location	
		_		

CONTENTS xvi

		7.2.3 Block distance from the tunnel	61
	7.3	Evaluation approach	61
	7.4	Results	62
	7.5	Interpretation and discussion	67
8	Fibi	re optic monitoring section: Data evaluation 1	69
	8.1	Distributed fibre optic sensing	
	8.2	Geological and hydrogeological conditions	
	8.3	Rock mass types	
	8.4	Primary stress state	
	0.1	8.4.1 General	
		8.4.2 Primary stress at the analysed section	
	8.5	Tunnelling method	
	0.0	8.5.1 Excavation sequence	
		8.5.2 Support	
		8.5.3 Work steps	
	0.6	•	
	8.6	Position of monitoring devices	
	8.7	Observed system behaviour: Geodetic measurements	
		8.7.1 Time-dependent displacements	
		8.7.2 Out-of-plane displacements	
		8.7.3 In-plane displacements	
	8.8	Observed system behaviour: DFOS	
		8.8.1 Strain in the circumferential and longitudinal direction	
		8.8.2 Evolution of strain with time	
		8.8.3 Strain rate	
	8.9	Observed system behaviour: Temperature	96
9	Fib	re optic monitoring section: Calibration case (3D)	01
	9.1	Limitations	02
		9.1.1 Time-dependent rock deformation	02
		9.1.2 Swelling	02
		9.1.3 Porewater pressure	02
	9.2	DFOS section: Strain components utilising a micromechanical model 2	03
		9.2.1 Neglecting thermal strain	04
		9.2.2 Neglecting shrinkage strain	05
	9.3	Burgers model	05
		9.3.1 Basic rheological models	07
		9.3.2 Combined rheological models	07
	9.4	•	10
		9.4.1 Modelling of system features	12
		9.4.2 Modelling of material behaviour	
		~	14
			15
			15
			15
		r o	16
		9.4.8 Creep time step	
		one creep time step	-

CONTENTS xvii

	9.5	Numerical input parameters	20
		9.5.1 Tunnel shape and size $\dots \dots \dots$	20
		9.5.2 Primary stress state	20
		9.5.3 Rock mass	20
		9.5.4 Backfill	25
		9.5.5 Shotcrete lining	25
		9.5.6 Rock bolts	33
	9.6	Evaluation approach	36
	9.7	Results	36
	9.8	Interpretation and discussion	40
10		,	43
	10.1	Limitations	
	10.2	Geological and hydrogeological conditions	
	10.3	Rock mass types	
	10.4	Primary stress state	
		10.4.1 General	
		10.4.2 Primary stress at the analysed section	
	10.5	Tunnelling method	
	10.6	Position of monitoring devices	
	10.7	Observed system behaviour: Geodetic measurements	
	10.8	Numerical model setup	
		10.8.1 Modelling of system features	
		10.8.2 Modelling of material behaviour	
		10.8.3 Mesh	
		10.8.4 Model size	
		10.8.5 Boundary conditions and initial state	
		10.8.6 Construction sequence	
	10.9	Numerical input parameters	
		10.9.1 Tunnel shape and size	
		v	60
			61
		9	67
			68
		**	68
			69
	10.12	Interpretation and discussion	71
11	Disc	ussion 2'	77
	11.1		77
	11.2	·	78
	11.3		79
	11.4		79
	11.5		81
	11.6		81
			81
		11.6.2 Tunnel support	
		**	

CONTENTS xviii

	11.6.3 Tunnelling sequence	284
12 Con	aclusion	285
Bibliog	graphy	287
Appen	dix A: Equations	317
A.1	Stress invariants	317
A.2	Strain invariants	317
A.3	Mohr-Coulomb failure criterion	318
A.4	Size of the yield zone in a homogeneous, isotropic rock mass	318
A.5	Elastic secondary tangential in-plane stresses around a circular opening in a	
	homogenous, isotropic medium	319
A.6	Elastic secondary tangential in-plane stresses around an elliptic opening in a	
	homogenous, isotropic medium	320
Appen	dix B: Some mechanical properties of rocks	321
В.1	Tensile strength	321
2.1	B.1.1 Johnston (1985)	
	B.1.2 Kluckner (2012)	
	B.1.3 Rostami et al. (2016)	
B.2	Dilation angle	
5.2	B.2.1 Terminology	
	B.2.2 Kluckner (2012)	
B.3	Poisson's ratio	
B.4	Young's modulus	
2.1	20446 2 4004444	0_0
Appen	dix C: Stiff block next to excavation (2D): Parametric study	329
C.1	Numerical model setup	
	C.1.1 Evaluation of constitutive model for matrix material	
	C.1.2 Evaluation of minimum in-plane model size	
	C.1.3 Evaluation of solve limit	337
	C.1.4 Evaluation of excavation method	342
C.2	Numerical input parameters	343
	C.2.1 Mechanical properties of model features	343
	C.2.2 Evaluation of interface stiffnesses	350
C.3	Results: Details	355
	C.3.1 In-plane block-matrix interface slip	355
	C.3.2 Shear strain increment	370
	C.3.3 Block deformation: Bending	385
	C.3.4 Block deformation: Change in the block height	391
	C.3.5 Block deformation: Change in the block width	393
	C.3.6 Block displacement	396
	C.3.7 Path of the largest secondary in-plane major principal stresses $\dots \dots$	400
	C.3.8 Shear strain increment along tunnel periphery	405
	C.3.9 Displacement of the tunnel periphery	411
	C.3.10 Yielded zones	425
	C.3.11 Block failure	438

CONTENTS				
C.3.12 In-plane stresses	457			
C.3.13 Orientation of in-plane stresses	472			

C.3.14 Elastic work	485
Appendix D: Fibre optic monitoring section: Data evaluation	497

Chapter 1

Introduction

This chapter starts with the research motivation (Section 1.1) based on which the research questions are formulated (Section 1.2 on p. 4). The next section (Section 1.3 on p. 5) details the methodology applied to work out answers to the questions. Section 1.4 (p. 6) shows the thesis structure and the main objectives of the thesis parts. The last section (Section 1.5 on p. 7) lists the research limitations.

1.1 Research motivation

On July 31st, 1994, at 2.45 a.m., the top heading of the heading *Leoben* collapsed at chainage 1,333.60 m. The heading is part of the 5,462 m long *Galgenberg* tunnel ([323, p. 7]), a two-track railway tunnel constructed from 1993 to 1995 ([361, p. 213]). The tunnel was divided into three headings, namely the top, the bench, and the invert. The cross section of the tunnel is approx. 110 m², and of the top heading approx. 60 m² ([363, p. 61]). Each round of the top heading was excavated and supported in four parts. When miners were applying shotcrete to the last quarter (i.e., lower right), the supported crown failed from the left shoulder up to 2 m above the right side of the top-heading invert and buried men and machine ([363, p. 62]) (cf. Fig. 1.1b). The collapse occurred at the end of the *Hinterberg* fault zone, which had to be crossed by the tunnel over a length of 383 m. There, the overburden was approx. 250 m ([361, p. 214]). A mass of approx. 700 m³ collapsed into the tunnel ([363, p. 62]) and filled approx. the last 8 m of the heading. This tragic occurrence with one fatality happened suddenly and without warning ([363, p. 63]). [362, Chapters 1, 3.2, 5]

The *Hinterberg* fault zone probably developed during a young oblique slip event. It is wedged in between two massive marble bodies ([323, p. 7]), separated by steep slickensides (cf. Fig. 1.2). The fault zone crosses the tunnel at an acute angle of approx. 30°. Its source rocks comprise imbricated graphitic and carbonate phyllites, green schists, and thinly bedded marbles ([36] in [361, p. 214]). The rocks are sheared and folded in a complex way. The alternation of soft, clayey gouges and variable fractured rock mass makes the fault zone extremely heterogeneous ([323, p. 7]). From the beginning of the fault zone in the SE to the end in the NW, the degree of fragmentation and the share of clayey fault gouge continuously increased ([363, p. 61]). Near the end, the collapse occurred. Here, miners had to cope with soil-like cataclasites and tectonic breccias. The fault gouge featured a low friction angle of 12...14° ([323, p. 7]). [362, Chapters 3.1, 3.3]

The round length of the top heading was 1 m. Miners used mainly excavators, and sometimes loosening blasting in very competent regions ([363, p. 61]). The support of the tunnel comprised

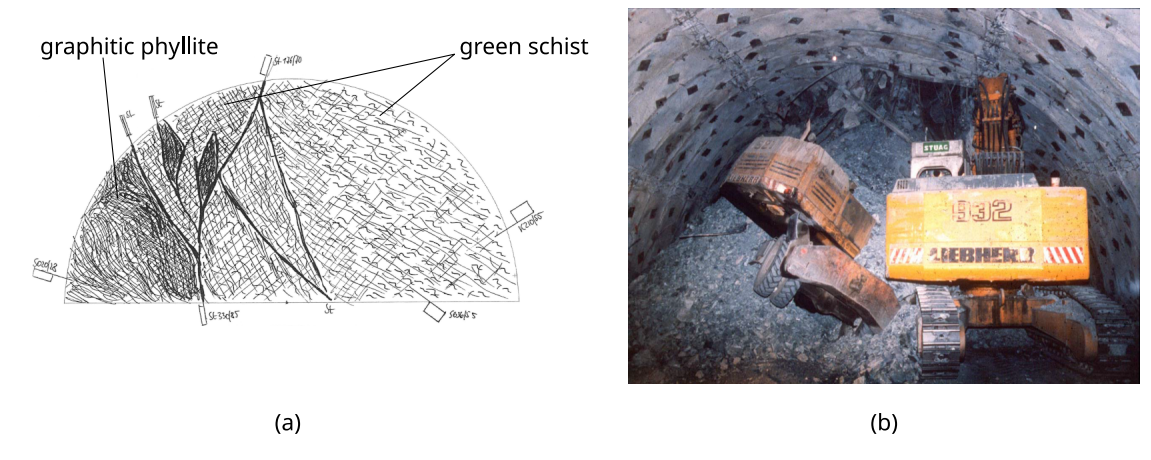


Figure 1.1: Galgenberg tunnel, heading Leoben: (a) Mapping of the tunnel face at chainage 1,331.60 m (modified from [363, Fig. 3, p. 61]; K...joint, S...foliation plane, St...slickenside). (b) Photograph of the collapse close to the end of the Hinterberg fault zone (from [361, Fig. 6, p. 215]).

a shotcrete lining (t=20 cm) with one layer of wire mesh, a lattice girder, 13 grouted bolts (l=6 m) installed radially approx. 1.3 m behind the face, and 14 grouted bolts (l=8 m) installed radially approx. 2.8 m behind the face. To cope with the large deformation of the rock mass, five open deformation gaps in the lining were foreseen. Thus, in the circumferential direction, the lining was separated into six segments. In the crown, 26 to 40 tube spiles (d=1.5 inches, l=4 m) are installed ahead of the face each round ([363, p. 62]). The tunnel face was temporarily supported with shotcrete, wire mesh, and load distribution beams fixed to grouted face bolts (nine pieces each 12 m long; before the collapse, the last series was installed at chainage 1328.60 m). [362, Chapter 4]

The site engineers monitored the system behaviour with three to five geodetic targets at the top heading. Recordings have been performed daily. The distance of measurement sections was approx. 10 m. Evaluations comprised time-displacement curves for each target and for each displacement component (i.e., horizontal, vertical, and longitudinal displacement). The level of final radial displacements within the *Hinterberg* fault zone ranged from 10 cm up to 100 cm ([361, p. 214]). [363, p. 62]

When heading through the *Hinterberg* fault zone and coming close to the cross section where the collapse occurred, interpreting the monitoring data did not show any signs of having a hazardous situation ahead. The interpretation approach has been state-of-the-art at that moment. The miners did not observe any abnormalities when excavating the round from chainage 1,332.60 m to chainage 1,333.60 m ([362, Chapter 5]). [363, p. 63]

Much effort was put into clarifying the reasons for this unforeseen event. The experts came up with several unfortunate circumstances the combination of which resulted in an unfavourable ground and system behaviour: (cf. [323, p. 7], [362, Chapter 7.3.2, 8, 10], [363, p. 60ff])

- extremely poor rock mass quality; the rock mass features a low shear strength and a strong fragmentation;
- the content of swellable clay minerals (i.e., Montmorillonite) ranges between 10% and 14% and is five to ten times higher than the average (<3%);
- large differences in the stiffnesses of geological features; the sudden alternations of relatively stiff and soft sheared rocks result in strongly heterogeneous conditions;

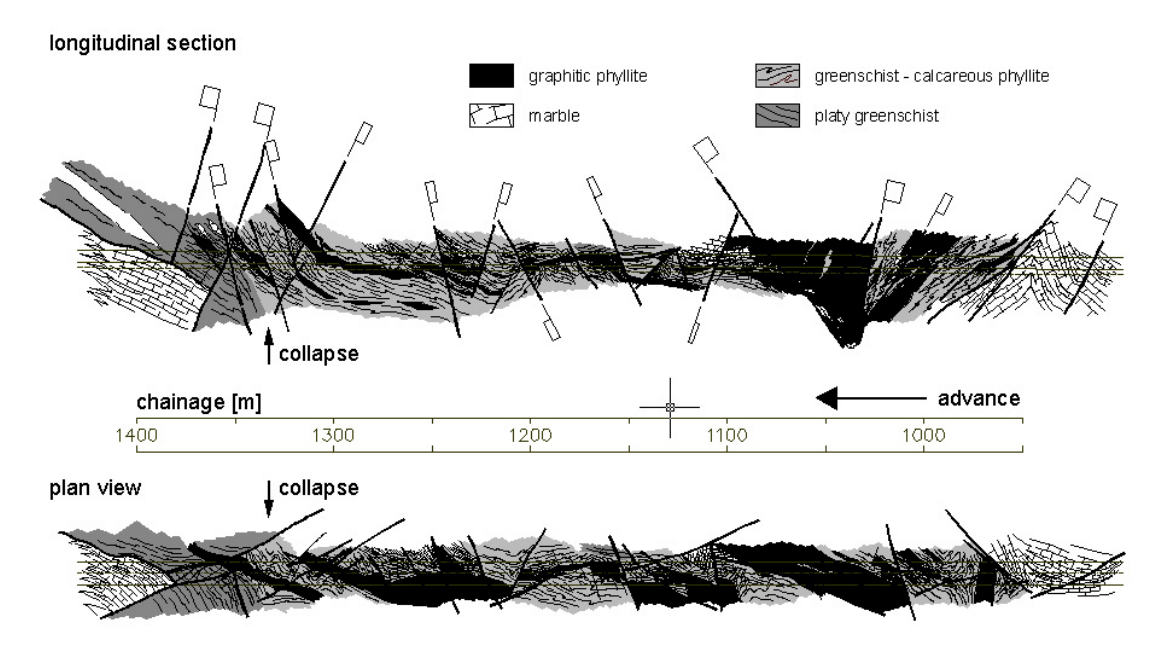


Figure 1.2: Galgenberg tunnel, heading Leoben: Internal structure of the Hinterberg fault zone (from [323, Fig. 8, p. 8].

- unfavourable crossing of faults, slickensides, and joints;
- unusual primary stresses (cf. Fig. 1.3): it is assumed that the fault material crept downhill limited by the stiff carbonate units on both sides of the fault zone; this resulted in an arching of the stresses where the carbonate units act as abutment; particularly close to the boundaries of the fault zone the principal stresses are not vertical and horizontal as initially assumed but rotated; the assumption of the primary stresses being rotated bases on the evaluation of the ratio of the displacement of the crown in the longitudinal direction to the crown settlement;
- unfavourable primary stresses: it is assumed that the rotated primary stresses favoured slip along weakness planes, which dip medium-steep to steep close to where the collapse occurred; in particular along slickensides, which are often parallel to sub-parallel to the foliation planes;
- the bonding of grouted bolts (standard type at that time) suffered from initial high strain rates ([361, p. 215]).

One circumstance probably contributed most to this worst-case scenario: at the location of the collapse, the rock block of relatively competent green schist is enclosed by zones of strongly tectonised graphitic phyllites and by steeply dipping faults (cf. Fig. 1.1a and Fig. 1.2; in the latter graph, arrows highlight the location of the collapse). [362, Chapter 8]

When the heading approached this rock mass zone, the stresses concentrated in the relatively stiff green schist block rather than the in fault gouge. It was assumed that at a particular moment the stiff block outside (!) the excavation area failed in a brittle manner ([252, p. 31], [361, p. 215]). The weak material surrounding the block could not take the additional load and sheared as well. [362, Chapter 8]

For future headings through such complex rock masses, the experts proposed several measures to be applied on site if necessary: (cf. [147, p. 86], [362, Chapter 9.2], [363, p. 66])

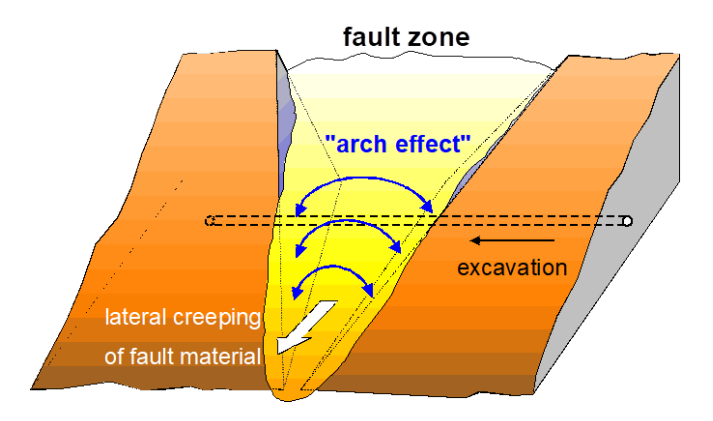


Figure 1.3: Galgenberg tunnel, heading Leoben: Development of arch type primary stress in the Hinterberg fault zone; simplified model (from [323, Fig. 9, p. 8]).

- installation of radial rock bolts as close to the tunnel face as possible; this increases the probability of having discontinuities or shear surfaces close to the tunnel face dipping medium-steeply to steeply also crossed by some bolts;
- installation of rock bolts which allow for repeated grouting to prevent bonding loss if the initial deformation is large, and to compensate for any loosening;
- use of grouting material which hardens rapidly;
- Use of rock bolts with a profile which reduces the potential of shearing of the fresh grout;
- reduction of the top-heading height to increase face stability;
- installation of yielding elements within the deformation gaps to allow for transferring normal loads from one shotcrete segment to the other without damaging the shotcrete lining;
- final ring closure within 100 m behind the heading tunnel face.

All those measures increase the system stability. However, their main purpose is to decrease the level of deformation. With increasing deformation, due to the stiffness contrast, the stresses concentrate in the stiff blocks (cf. [362, Chapter 9.2] and [361, p. 215]). Such stress concentrations can then lead to brittle failure in the stiffer features accompanied by additional displacements of the weaker material ([252, p. 23]). According to the experts, brittle failure contributed significantly to the collapse described here and its suddenness surprised all involved ([360, p. 4, 7]). Thus, in heterogeneous rock masses, [323, p. 10] suggest to reinforce also larger stiffer features or sections in order to prevent failure, which would lead to stress redistribution to weaker sections again.

When heading through the *Hinterberg* fault zone, several stiff blocks were crossed, without reported major problems. Anyway, at the end of the fault zone, a stiffer feature was probably the key aspect triggering the motion which resulted in the incident detailed here. As large-volume overbreaks were reported in other tunnels associated when approaching stiffer rock masses (cf., e.g., [109, 270]), this is a subject worth investigating in more detail.

1.2 Research questions

Having the incident at the *Galgenberg* tunnel in mind, and the task of a geotechnical site engineer to prevent such by realising the problematic situation in time, the question arises whether the

latter is even possible. To do so, the engineer must have a good idea about the expected behaviour of the ground and the system¹ when it comprises stiff blocks. The thesis limits the problem investigation to two key questions:

- 1. What is the ground behaviour when approaching a single stiff block embedded in a weak matrix?
- 2. Is it possible to notice the existence of the block when analysing displacement data of monitoring cross sections farther behind when approaching the block?

Since engineers should strive for excavation and support concepts following the principle of as much as needed but as little as possible, reflections about the concepts are to be addressed as well.

1.3 Methodology

Four main steps need to be completed to create knowledge to answer the questions: The first step requires a literature research on the characteristics of weak rock masses and stiff blocks to identify suitable geometric and mechanical parameters for theoretical considerations and analyses. In the next step, a parametric study is performed simulating the excavation of a circular tunnel in a weak matrix numerically with quasi-two-dimensional models. Next to the tunnel side wall, there is an elliptic stiff block embedded in the matrix. The study varies the size of the block, its distance to the tunnel, the size of the yield zone, the stiffness and strength contrast between the rock mass features (i.e., matrix and block), and the primary stress state. The maximum block size considered equals the tunnel size. Note that in nature the occurrence of smaller blocks is higher than of larger blocks. Thus, it is more likely that a tunnel drive comes close to a smaller block. Results are evaluated and interpreted extensively to identify all phenomena making up a good basis for all considerations in this thesis but also for follow-up studies dealing with similar scenarios. The simulation of one case of the parametric study in three dimensions (supplementary study) completes the second step. All cases apply the Mohr-Coulomb model to the rock mass features. Both the quasi-two-dimensional and the three-dimensional simulations allow to establish the main hypotheses. In the last step, a real tunnel drive approaching a stiff block is simulated numerically in three dimensions (validation case). The results are then compared with the behaviour observed at the construction site and, based on that, the hypotheses are discussed. A realistic simulation of a tunnel drive and the resulting ground and system behaviour requires knowledge about the characteristics of all system features. Next to the ground, that are, for example, the primary stresses and the support. Because the former can usually be estimated only, at least the latter should be well known to reduce the modelling uncertainties. Here, in particular, the shotcrete lining with its time-dependent behaviour is difficult to model. Thus, in the step next to last, real strain data from a monitoring cross section of a conventional tunnel drive, of which the lining is equipped with a distributed fibre optic sensing system, is used to calibrate a Burgers-Mohr model (calibration case). The model enables the calculation of the elastic, plastic, and creep strain of the shotcrete.

All numerical simulations are performed with the Finite Difference software package FLAC3D ([178]). Tab. 1.1 lists the constitutive models to simulate the material behaviour of the main elements in the numerical studies in this thesis.

¹The ground behaviour is the "Reaction of the ground to the excavation of the full profile without consideration of sequential excavation and support". In contrast, the system behaviour is the "Behaviour resulting from the interaction between ground, excavation, and support". [290, p. 5]

Table 1.1: Methodology: Constitutive models used for the main elements in the numerical studies with FLAC3D ([178]).

			Constit		nodel		Thesis
Simulation	Element	BM	HSS	MC	UJ	CS	section
Parametric study (quasi-2D):							
Evaluation model setup	rock mass		x	x		X	6.1, C.1
Evaluation input parameters	rock mass			\mathbf{x}		X	6.2, C.2
Simulations	rock mass			\mathbf{x}		X	6.1, 6.2
Supplementary study (3D):							
Simulations	rock mass			\mathbf{x}		X	7.1, 7.2
Calibration case (3D):							
Evaluation Burgers model	shotcrete element	x					9.3
Simulations	rock mass			\mathbf{x}	\mathbf{X}	X	9.4, 9.5
	shotcrete lining	x				X	
Validation case (3D):							
Simulations	rock mass			\mathbf{x}	X	X	10.8, 10.9
	shotcrete lining	x				X	

Zones, volume elements:

BM ...Burgers-Mohr model

HSS ... Hardening Soil Small model; in FLAC3D implemented as Plastic Hardening (PH) model with small-strain stiffness option

MC ... Mohr-Coulomb model with tension cut-off

 ${
m UJ}$... Ubiquitous Joint model utilising MC for both the zones and the weakness planes

Interfaces:

CS ... Coulomb sliding with tensile and shear bonding

1.4 Thesis structure and objectives

Differences in the stiffness between geological features next to each other can be large in fault zones which are usually heterogeneous (cf. example case introduced in Section 1.1 on p. 1). Some fault zone material may be of the block-in-matrix type comprising larger stiffer blocks embedded in a weaker matrix material. Block-in-matrix rocks can form in different ways. For example, by weathering of initially solid rock, by lithification of sedimentary rock, or by solidification of igneous rock. But they can form also in brittle fault zones when shear concentrates, gradually comminuting rock mass zones to weak matrix material and sparing stronger rock blocks. The thesis focuses on the latter and, thus, Chapter 2 (p. 9) briefly gives some information on fault zones for a general understanding and an introduction to block-in-matrix rock types.

The parametric study and the supplementary study aim to simulate a possible scenario of a single stiff block next to a circular excavation. Chapter 3 (p. 19) summarises some published rock and rock mass property ranges and examples of geometric and mechanical properties of block-in-matrix rocks. Based on these, later in Chapter 6, reasonable ranges of the input parameters for the studies are established.

The calibration case (Chapter 9) and the validation case (Chapter 10), both simulating a real tunnel drive, comprise also the modelling of the shotcrete lining. To get an idea about the material behaviour of shotcrete, Chapter 4 (p. 45) describes the ageing process of shotcrete (or concrete) accompanied by the development of strength and stiffness, and the main strain components when being loaded (e.g., creep strain). It also reports on how some other researchers modelled shotcrete analytically or numerically. The summary facilitates the determination of reasonable input parameters for the calibration of the shotcrete modelling approach in Chapter 9.

Chapter 5 (p. 69) introduces the thermo-chemo-mechanical shotcrete model established by *Prof. Christian Hellmich* (Vienna University of Technology, Vienna, Austria) and

colleagues, which is implemented in the software suite TUNNEL:Monitor ([142]). The implementation is required to split the total strain measured at site with the distributed fibre optic sensing system (Chapter 8) into the individual strain components of the shotcrete lining (e.g., elastic strain, creep strain, shrinkage strain). They are later used for the calibration of the shotcrete modelling approach (Chapter 9). Introducing the shotcrete model by *Hellmich* allows for the recognition of phenomena the strain components actually accommodate and of those that remain unconsidered.

In the next chapter (Chapter 6 on p. 81), the quasi-two-dimensional parametric study is presented. The text covers the setup of the numerical model, the identification of the material parameters, the approaches to evaluate the simulation results, a summary of the results, and interpretations and discussions. Chapter B.4 (p. 329) in the appendix gives a more detailed description of the results. The parametric study and the three-dimensional supplementary study (Chapter 7 on p. 159) disclose the theoretical ground behaviour when a tunnel excavation takes place near a stiff block.

Chapter 8 (p. 169) illustrates the strain data recorded with the distributed fibre optic sensing system. It also comprises the evaluation and interpretation of the deformation behaviour of the shotcrete lining. The latter helps to set up the calibration model (Chapter 9) adequately and serves for a comparison with the numerical results.

The next chapter (Chapter 9 on p. 201) comprises two main parts: the calibration of the Burgers-Mohr model for the simulation of the shotcrete behaviour and the simulation run of the calibration case and related evaluations and interpretations.

The calibrated material model and applicable model settings are then used to adjust the validation case in Chapter 10 (p. 243). Results from the simulation run validate the hypotheses made up in Chapter 6 and Chapter 7. The outcome is described accordingly.

The discussion (Chapter 11 on p. 277) and the conclusion (Chapter 12 on p. 285) complete the main part of the thesis.

In the appendix (p. 317), four chapters give additional information for the interested reader: Chapter 12 (p. 317) lists some analytical equations. Chapter A.6 (p. 321) relates to Chapter 3 (p. 19) in the main part of this thesis and comprises detailed information on researched mechanical rock properties. Results of numerical simulations to evaluate model setups and input parameters as well as an extended evaluation of the results of the quasi-two-dimensional parametric study are given in Chapter B.4 (p. 329). It relates to Chapter 6 (p. 81) in the main part. And some more evaluations of the strain data measured with the distributed fibre optic sensing system (cf. Chapter 8 on p. 169) can be found in Chapter C.3.14 (p. 497).

1.5 Research limitations

The studies analyse scenarios with a single stiff block near the excavation. They do not deal with the interaction of two or more blocks like in block-in-matrix-rocks of fault zones. Anyway, the single-block scenario can also exist in block-in-matrix rocks. Thus, the parameter research takes block-in-matrix rocks into account.

Considerations are limited to brittle faults in the upper crust and to deep tunnels (i.e., overburden > approx. three times the tunnel diameter) excavated conventionally. The case studies neglect any influence of the topology on the primary stresses or effects the excavation has on the surface and vice versa.

Since site engineers have to identify a hazardous situation ahead within a short period, only the

first days after the excavation are of interest. Effects of any water drawdown are less important. In the case studies, the reported ingress of water is little. But, in particular in the calibration case (cf. Chapter 9), porewater pressure and groundwater flow may have affected the ground behaviour. Anyway, water is neglected in the simulations. All strength parameters cited in the thesis are drained strengths (i.e., from tests on non-saturated material under drained conditions).

The numerical simulations are static analyses. The accumulation of elastic energy in the block is investigated in the theoretical studies but consequences in terms of dynamic loads when the block fails are briefly discussed but not calculated.

Some interpretations of results introduce effects a different tunnel shape has on the tunnel displacement pattern but the theoretical studies do not vary the tunnel shape. It is always circular.

The thesis focuses on the risks a stiff block introduces when a tunnel drive approaches it. However, a block can also reduce the rock mass deformation if it remains intact. The positive effect on the tunnel is not discussed.